P-wave traveltime inversion in weakly anisotropic media: a preliminary study

Bohuslav Růžek and Ivan Pšenčík

Institute of Geophysics, Acad. Sci. of Czech Republic, Boční II, 141 31 Praha 4, Czech Republic. E-mail: b.ruzek@ig.cas.cz; ip@ig.cas.cz

Abstract

There is an increasing interest in seismic exploration in studying media of lower anisotropic symmetry. It is therefore necessary to study traveltime inversion of data obtained in such media using various experiments in order to find out, which parameters and under what conditions can be retrieved from observed traveltime data. We concentrate on a VSP (vertical seismic profiling) experiment, which provides a good angular illumination, and we study the inversion on several sets of synthetic P-wave traveltime data in homogeneous models of orthorhombic media. As expected, results of preliminary tests indicate sensitivity to the quality of the angular illumination of the model and strong sensitivity to noise.

1 Introduction

Several attempts to study possibilities of traveltime inversion in anisotropic media of symmetry lower than transversely isotropic have been made in the past. Let us mention Chapman and Pratt (1992), Pratt and Chapman (1992), Mensch and Farra (2002). In these papers, the authors faced problems with insufficient illumination of the medium, problems with the determination of incomplete sets of parameters specifying the medium and problems with distinguishing effects of anisotropy from effects of inhomogeneity. In order to simplify their study, the authors resorted either to 2D specifications of their models or to the use of the so-called factorized anisotropy concept (Červený, 1989), which reduces considerably the number of parameters required for the specification of the model.

Our long-term plan is the traveltime inversion for 3D inhomogeneous media of arbitrary anisotropy. Since we are well aware of all the problems faced by the above-mentioned authors, we start with very simple tests. We concentrate on direct P waves propagating in a homogeneous, but generally anisotropic medium. In fact, our test models are of orthorhombic symmetry, but because we consider also the cases, in which planes of symmetry of the orthorhombic medium deviate from coordinate planes, we must consider a general anisotropy in the inversion process. We use a vertical seismic profiling (VSP) configuration, which provides relatively good angular illumination of the model. We consider a borehole with receivers situated in it, and several straight profiles on the surface with shot points along them. "Observed" traveltime data are generated by the program package ANRAY (Gajewski and Pšenčík, 1990). Since the medium is homogeneous, there

Seismic Waves in Complex 3–D Structures, **24** (2014), 17–34 (ISSN 2336–3827, online at http://sw3d.cz)

is no need for ray tracing in the inversion process. Rays are straight lines connecting sources and receivers and the only quantity in the traveltime formula, which is affected by the parameters of the medium, is the ray velocity. We use leading terms of the weak-anisotropy approximation of exact expressions for the ray velocity. In this approximation, the ray velocity is expanded in terms of small parameters characterizing deviation of anisotropy from isotropy. Farra and Pšenčík (2014) offer three such expressions (eqs (5)-(7)) of varying accuracy for the ray velocity in anisotropic media of arbitrary symmetry. The formulae are expressed in terms of weak-anisotropy (WA) parameters, which characterize the deviations of the considered anisotropic medium from a reference isotropic medium. In order to keep the relations between the ray velocity and WA parameters linear, we use the least accurate approximation, eq. (5) of Farra and Pšenčík (2014). Adopting this approximation, we assume that the ray velocity equals the phase velocity not only in its size (this is true in the first-order approximation, see, e.g., Backus, 1965), but also in direction. In fact, as Farra and Pšenčík (2014) show, the directions of the ray-velocity and phase-velocity vectors might differ quite significantly. Nevertheless, as we show in this study, even with this rough approximation, we can obtain reasonable results (if weak-anisotropy assumption is satisfied). In the following, we thus use only phase velocity.

Least-square procedure (Press et al., 1986), specifically pseudoinverse (Aster et al., 2005) is used to solve the inverse problem. Inversion is tested on traveltime data corresponding to four models, two of anisotropy of about 12%, the other two of anisotropy of about 25%. As a measure of P-wave anisotropy strength, we use the relation $2(V_{max} - V_{min})/(V_{max} + V_{min}) \times 100\%$.

In Section 2, we present two different expressions for the P-wave phase velocity c in terms of 15 P-wave WA parameters, which specify the most general anisotropic media. One expression is for c^2, the other for c^{-1}. The latter one is closer to the form, in which the velocity in inhomogeneous media is considered. It is important to note that the formula for c^{-1} can be obtained by the linearization of the expression for c^2. The expression for c^{-1} thus represents a less accurate approximation of the phase velocity. The two expressions for the phase velocity are used in Section 3 to formulate the inverse problem. In addition, it is also shown there how to estimate errors in the determination of WA parameters. The models used and the experiment configuration are described in Section 4. Results of preliminary test are then shown and discussed in Section 5. Section 6 contains conclusions and indicates future plans.

2 Linear equations for the weak-anisotropy parameters

The presented inversion is based on the solution of two systems of linear equations. The first has the following form:

$$c^2(\mathbf{n}) = r^2/t^2 \ . \tag{1}$$

In (1), the symbol t is the "observed" traveltime; in our case it is traveltime computed by the program package ANRAY, the symbol r denotes the corresponding source-receiver distance and $\mathbf{n}$ a unit vector parallel to the source-receiver direction. The symbol $c(\mathbf{n})$

represents the first-order phase velocity. It is given by the equation (Pšenčík and Farra, 2005):

$$\begin{aligned} c^2(\mathbf{n}) = \alpha_0^2\Big(1 + 2(\epsilon_x n_1^4 + \epsilon_y n_2^4 + \epsilon_z n_3^4 + \delta_x n_2^2 n_3^2 + \delta_y n_1^2 n_3^2 + \delta_z n_1^2 n_2^2) \\ +4[(\epsilon_{15} n_3 + \epsilon_{16} n_2) n_1^3 + (\epsilon_{24} n_3 + \epsilon_{26} n_1) n_2^3 + (\epsilon_{34} n_2 + \epsilon_{35} n_1) n_3^3 \\ +(\chi_x n_1 + \chi_y n_2 + \chi_z n_3) n_1 n_2 n_3]\Big) \ . \end{aligned} \tag{2}$$

The coefficients of n_i in equation (2) are the 15 P-wave weak-anisotropy (WA) parameters specifying anisotropy of an arbitrary symmetry. They have the following meaning:

$$\begin{aligned} &\epsilon_x = \tfrac{A_{11}-\alpha_0^2}{2\alpha_0^2}, \quad \epsilon_y = \tfrac{A_{22}-\alpha_0^2}{2\alpha_0^2}, \quad \epsilon_z = \tfrac{A_{33}-\alpha_0^2}{2\alpha_0^2}, \\ &\delta_x = \tfrac{A_{23}+2A_{44}-\alpha_0^2}{\alpha_0^2}, \quad \delta_y = \tfrac{A_{13}+2A_{55}-\alpha_0^2}{\alpha_0^2}, \quad \delta_z = \tfrac{A_{12}+2A_{66}-\alpha_0^2}{\alpha_0^2}, \\ &\epsilon_{15} = \tfrac{A_{15}}{\alpha_0^2}, \quad \epsilon_{16} = \tfrac{A_{16}}{\alpha_0^2}, \quad \epsilon_{24} = \tfrac{A_{24}}{\alpha_0^2}, \quad \epsilon_{26} = \tfrac{A_{26}}{\alpha_0^2}, \quad \epsilon_{34} = \tfrac{A_{34}}{\alpha_0^2}, \quad \epsilon_{35} = \tfrac{A_{35}}{\alpha_0^2}, \\ &\chi_x = \tfrac{A_{14}+2A_{56}}{\alpha_0^2}, \quad \chi_y = \tfrac{A_{25}+2A_{46}}{\alpha_0^2}, \quad \chi_z = \tfrac{A_{36}+2A_{45}}{\alpha_0^2}. \end{aligned} \tag{3}$$

The symbols $A_{\alpha\beta}$ denote density-normalized elastic parameters in the Voigt notation. The quantity α_0 in (2) and (3), with the dimension of velocity, can be understood as a P-wave velocity of a reference isotropic medium. Let us emphasize that WA parameters (3) depend on the choice of α_0 while the expression (2) with WA parameters (3) is independent of it. The quantity α_0 should be chosen so that it makes all WA parameters small. In experiments with prevailingly vertical wave propagation, α_0 should be chosen so that ϵ_z equals zero, i.e., $\alpha_0 = A_{33}$. In this case, the WA parameters represent linearized version of Thomsen (1986) parameters, generalized to media of arbitrary anisotropy. Because our experiments include propagation directions from horizontal to vertical, it is reasonable to choose α_0 close to an average velocity in the model. Change of the value of α_0 after the inversion represents no problems, it requires just a simple manipulation with WA parameters (3).

Besides expression (2), we also consider an alternative expression for $c^{-1}(\mathbf{n})$, whose form is closer to the form, in which is the velocity used in inhomogeneous media:

$$\begin{aligned} c^{-1}(\mathbf{n}) = \alpha_0^{-1}\Big(1 - (\epsilon_x n_1^4 + \epsilon_y n_2^4 + \epsilon_z n_3^4 + \delta_x n_2^2 n_3^2 + \delta_y n_1^2 n_3^2 + \delta_z n_1^2 n_2^2) \\ -2[(\epsilon_{16} n_2 + \epsilon_{15} n_3) n_1^3 + (\epsilon_{24} n_3 + \epsilon_{26} n_1) n_2^3 + (\epsilon_{35} n_1 + \epsilon_{34} n_2) n_3^3 \\ +(\chi_x n_1 + \chi_y n_2 + \chi_z n_3) n_1 n_2 n_3]\Big). \end{aligned} \tag{4}$$

In this case, equations for the inversion have the form:

$$c^{-1}(\mathbf{n}) = t/r \ . \tag{5}$$

Combination of equations (1) and (2) or (4) and (5) results in a system of linear equations for the determination of 15 unknown WA parameters from N observed traveltimes t_i corresponding to source-receiver distances r_i in directions $\mathbf{n}_i$.

3 Inversion scheme

In order to understand the potential of anisotropic traveltime inversion to estimate WA parameters, it is advantageous to use linear algebra wherever it is possible. In such a case,

standard procedures like singular value decomposition or pseudoinverse (see, e.g., Aster et al., 2005; Press et al., 2007) can be used. We use pseudoinverse in this study. System of equations (1) for each observation can be rewritten in the matrix notation:

$$\mathbf{G}\mathbf{m} = \mathbf{d}. \tag{6}$$

In (6), $\mathbf{G}$ represents the $N \times M$ forward operator matrix. N is the number of observations and M is the number of sought WA parameters, i.e., $M = 15$. The rows of matrix $\mathbf{G}$ have the following form:

$$\begin{aligned}(&n_1^4 \quad n_2^4 \quad n_3^4 \quad n_2^2 n_3^2 \quad n_1^2 n_3^2 \quad n_1^2 n_2^2 \quad 2n_1^3 n_3 \quad 2n_1^3 n_2 \quad 2n_2^3 n_3 \\ &2n_2^2 n_1 \quad 2n_3^2 n_2 \quad 2n_3^3 n_1 \quad 2n_1^2 n_2 n_3 \quad 2n_1 n_2^2 n_3 \quad 2n_1 n_2 n_3^2).\end{aligned} \tag{7}$$

Each row in matrix $\mathbf{G}$ corresponds to one particular ray (connection of source and receiver). Symbol $\mathbf{m}$ denotes the vector of model parameters to be determined. In our case, it consists of 15 P-wave WA parameters and has the form:

$$\mathbf{m} \equiv (\epsilon_x, \epsilon_y, \epsilon_z, \delta_x, \delta_y, \delta_z, \epsilon_{15}, \epsilon_{16}, \epsilon_{24}, \epsilon_{26}, \epsilon_{34}, \epsilon_{35}, \chi_x, \chi_y, \chi_z)^T. \tag{8}$$

We take into account all 15 WA parameters specifying general weak anisotropy because for rotated orthorhombic symmetry all 15 WA parameters in (8) can be non-zero. Vector $\mathbf{d}$ contains "observed" traveltimes t_i and source-receiver distances r_i. Because we consider reference velocity used for the definition of WA parameters (3) as known, vector $\mathbf{d}$ also contains α_0. Vector $\mathbf{d}$ has thus the form:

$$\mathbf{d} \equiv \Big(\frac{1}{2}(\frac{r_1^2}{\alpha_0^2 t_1^2} - 1),\ \frac{1}{2}(\frac{r_2^2}{\alpha_0^2 t_2^2} - 1),\ ....,\ \frac{1}{2}(\frac{r_N^2}{\alpha_0^2 t_N^2} - 1)\Big)^T. \tag{9}$$

Reference velocity α_0 can also be considered as an additional unknown satisfying certain prescribed conditions. For example, α_0 can be sought so that it makes some of WA parameters, say, e.g., ϵ_z, zero. It can also be chosen so that it leads to the minimum norm of WA parameters. In our tests, we use it constant, close to an average velocity.

Equation (5) gives rise to a system of equations, which can be again rewritten to the form (6).

Using all available data, equation (6) can be solved by pseudoinverse (e.g., Aster et al., 2005; Press et al., 2007):

$$\mathbf{m} = \mathbf{G}^\dagger \mathbf{d}. \tag{10}$$

Here $\mathbf{G}^\dagger$ denotes pseudoinverse of matrix $\mathbf{G}$.

The simplest way how to asses errors of WA parameters is to transform the data covariance matrix $\mathbf{C}_d$ to the model covariance matrix $\mathbf{C}_m$:

$$\mathbf{C}_m = \mathbf{G}^{\dagger T} \mathbf{C}_d \mathbf{G}^\dagger. \tag{11}$$

Since we do not know the data covariance matrix $\mathbf{C}_d$ exactly, we must use its approximation. We choose $\mathbf{C}_d$ as follows:

$$\mathbf{C}_d \approx \sigma^2 \mathbf{I}. \tag{12}$$

Here $\mathbf{I}$ is 15×15 identity matrix. The value of the parameter σ can be determined using χ^2 statistics of residuals $\mathbf{r} = \mathbf{d} - \mathbf{Gm}$ with number of degree of freedom $\nu = N - M$: since we have

$$\nu^{-1}\mathbf{r}^T\mathbf{C}_d^{-1}\mathbf{r} = \nu^{-1}\sigma^{-2}\mathbf{r}^T\mathbf{r} \approx 1, \tag{13}$$

we get

$$\sigma = \sqrt{\nu^{-1}\mathbf{r}^T\mathbf{r}}. \tag{14}$$

Using equation (11), we can thus estimate the model covariance matrix $\mathbf{C}_m$. Square roots of diagonal elements of $\mathbf{C}_m$ then represent individual errors of WA parameters.

4 Configuration of experiments and models

We consider a Cartesian coordinate system x, y, z, with the z-axis vertical, positive downwards. The x- and y-axes are horizontal, chosen so that the coordinate system is right-handed. In this system we use a VSP configuration with four receivers situated in a borehole parallel to the z-axis and passing through the origin of the coordinate system, see Figure 1. The receivers are situated at depths of 0.1, 0.3, 0.6 and 0.9 km. There are 7 surface profiles running from the borehole with 20 source points situated on each profile. The first profile is parallel to the x-axis, with azimuth $\varphi = 0$ rad. The remaining profiles have azimuths $\varphi = 1, 2, ...6$ rad. The sources are distributed on the profiles regularly with the step of 0.01 km, starting from 0.01 km. The most distant source is thus 0.2 km from the borehole. Generally, we have thus at our disposal 560 "observations", i.e., $N = 560$. Because we seek $M = 15$ WA parameters, the degree of freedom $\nu = N - M = 545$.

We use two homogeneous orthorhombic media. Anisotropy strength of the first one is about 12%, anisotropy of the other one is about 25%. The latter medium is the medium proposed by Schoenberg and Helbig (1997). Both models are used in a "non-rotated" and "rotated" version. In the non-rotated version the planes of symmetry of the considered model are parallel with the coordinate planes. The WA parameters of both models in the non-rotated version are given in Table 1. The reference velocity α_0 is chosen to be 2.44 km/s. This value is close to the vertical velocity in model with anisotropy of about 25%, which makes the WA parameter ϵ_z very small in this case.

Model	ϵ_x	ϵ_y	ϵ_z	δ_x	δ_y	δ_z
12%	0.193	0.211	0.128	0.277	0.237	0.342
25%	0.256	0.326	-0.001	0.075	-0.085	0.337

Table 1: Parameters of the non-rotated models used in tests; $\alpha_0 = 2.44$ km/s.

In the rotated version of the 12% anisotropy medium, we rotated it anticlockwise by 45^o around the z-axis. Afterwards, we rotated the medium anticlockwise by 30^o around the new y-axis. For the rotated 25% medium, we made only anticlockwise rotation by 30^o around the y-axis. In the following, we work with four models:

Model A1 - non-rotated model of 12% anisotropy;

Model A2 - rotated model of 12% anisotropy;

Model A3 - non-rotated model of 25% anisotropy;

Model A4 - rotated model of 25% anisotropy.

We are inverting data for the above 4 models under various conditions. Beside noise-free data, we also invert data with random Gaussian noise, data with the shallowest receiver removed, data with reduced number of profiles, with profiles with azimuths $\varphi = 1, 3, 5$ rad omitted.

5 Discussion of results

Figure 1 shows measurement configuration and 560 rays connecting 20 sources on each profile on the surface with 4 receivers in the borehole. Sources are distributed regularly along 7 radial profiles whose azimuths are $k\pi$ radians, k=0, 1, ..., 6. Totally there are 560 rays available. The rays from shots located close to the borehole are nearly vertical. The rays from shots at the ends of profiles to the shallowest receiver make an angle of about 26^o with horizontal. Thus nearly horizontal rays are missing.

Since we are inverting a linear system (see eq. (6)) whose matrix $\mathbf{G}$ has the rank 15 and the dimension of $\mathbf{m}$ is also 15, the only source of errors (if no noise is added to observed data) is the inconsistency of the data vector $\mathbf{d}$ with the used model, specified by eq. (2). We present this inconsistency in the form of histograms of relative traveltime errors $(t_{obs} - t_{cal})/t_{cal}$ in Figure 2. In the plot at the top left, no additive noise is applied. In an ideal case, the histogram would have delta function shape. But it has not. It is because t_{obs} is an exact traveltime calculated by the ANRAY code while t_{cal} is calculated approximately using eq. (2). As mentioned in Introduction, using eq. (2), we ignore the difference in orientation of phase-velocity and ray-velocity vectors, which might be significant, see Farra and Pšenčík (2014). Despite this, the top left plot indicates that eq. (2) represents a reasonable approximation. The remaining histograms (top right and bottom), correspond to data vector $\mathbf{d}$ distorted by additive Gaussian noise with magnitudes 1 ms (upper right), 2 ms (bottom left) and 5 ms (bottom right). From comparison of the histogram corresponding to data without noise with histograms corresponding to noisy data, it is obvious that the application of even very low noise dominates over the mismodelling effect and the histograms attain the well-known bell-shaped forms. These data are the subject of inversion.

In Figure 3, we present results of inversion of noise-free data (top left) and of data subject to increasing Gaussian noise for model A1, it is for model of anisotropy of about 12% with planes of symmetry parallel to the coordinate planes. Although the model is described by 6 P-wave WA parameters and 3 Euler angles (all the angles are zero in this particular case), we invert for 15 WA parameters, see eq. (3), assuming general anisotropy. Exact values of WA parameters are marked by black squares, estimated values by red crosses. Red bars indicate estimated errors (eq. (11)) of the corresponding WA parameters.

In the top left plot (noise-free data) we can observe a perfect fit of inverted and exact parameters. The error bars are so small that they are invisible. Inversion perfectly detected that the medium is orthorhombic (all extra WA parameters are zero). Situation changes when data with noise are considered. There are some parameters, which remain well determined and whose error bars are small: ϵ_x, ϵ_z, ϵ_{34}, ϵ_{35}, χ_z. Remaining parameters are, however, affected by the noise quite significantly. Generally, best estimated parameters are those, which are related to coordinate axes, along which observations exist. This concerns partially x- and completely z-axes. In the former case, the profile of azimuth $\varphi = 0$ rad is parallel to the x-axis, but rays make a certain angle with it. In the latter case, rays from sources closest to the borehole and recorded at deeper receivers are nearly vertical and thus nearly parallel to the z-axis. It is thus not surprising that ϵ_z is estimated very well and ϵ_x better than ϵ_y. Parameter ϵ_x characterizes propagation along the x-axis, ϵ_y characterizes propagation along the y-axis. Rays are closer to the x-axis than to the y-axis. The worst estimated WA parameter is δ_z followed by χ_x, χ_y, ϵ_{16}, ϵ_{26} and ϵ_{24}. Note that even for the lowest level of noise, the exact values of some parameters lie outside error bars of the estimated values.

Figure 4 shows the same as Figure 3, but for model A2, i.e., for rotated orthorhombic medium. It means that some WA parameters, which are zero for orthorhombic medium with planes of symmetry parallel to the coordinate planes, are non-zero in this case. Inversion of noise-free data leads, even in this case, to a perfect fit of inverted and exact WA parameters. The division of WA parameters on well and worse inverted when data subject to noise are used, is similar as in Figure 3.

When comparing Figures 3 and 4, it might be surprising that the inversion of noisy data leads to slightly different results for non-rotated and rotated cases. This difference has two reasons. The basic reason is that although the level of noise is the same in both cases, their realizations are different. The other reason is related to the approximate character of the expression for the phase velocity. As mentioned above, the approximate P-wave phase velocity is always less or equal to exact one. It means that the quality of the approximation varies with direction. This, in turn, means that for the same direction, the quality of the approximation is generally different for the non-rotated and rotated models.

In Figure 5, we show results for the models A3 (top) and A4 (bottom), i.e., for anisotropy of about 25%, for noise-free data (left) and for data affected by 5 ms Gaussian noise (right). We can observe expected larger errors than in models A1 and A2. Misfit can be observed already for noise-free data.

In the following we show effects of omission of a receiver or profiles. We use Model A4 for this purpose with additive random Gaussian noise of 5 ms in data. In the left plot of Figure 6, we show results of inversion with the shallowest receiver at the depth of 0.1 km omitted. It means, in fact, that we reduce the illumination cone from $\sim 26 - 90^o$ to $\sim 56 - 90^o$. This has quite dramatic effect on the size of error bars. Note that the scale on the vertical axis is extended with respect to the plots in previous figures. In the right plot, we show results of inversion for omitted profiles of sources 1, 3 and 5 rad. We can see that the omission of 3 intermediate profiles has practically no effect. It means that the remaining 4 profiles are sufficient.

Finally, we show comparison of results of inversion obtained from eq. (1) with $c^2(\mathbf{n})$

given in (2) and from eq. (5) with $c^{-1}(\mathbf{n})$ given in (4). We again use Model A4, this time with random noise of 3 ms. Results for eq. (1) with (2) are shown in the left plot of Figure 7, results for eq. (5) with (4) are shown in the right plot. Surprisingly, results obtained with less accurate formula (4) look better than with formula (2). We decided, therefore, to perform the following test. We made 100 inversions with random Gaussian noise of 10 ms. Such results are more objective than just a single realization used in previous examples. Results are shown in Figure 8. Note again extension of the scale on the vertical axis. Results for eq. (1) with (2) can be seen again in the left plot, results for eq. (5) with (4) are shown in the right plot. These plots show very clearly which parameters can be estimated reliably and which cannot. Comparison of both plots confirms that less accurate formula (4) performs better than formula (2). From 100 inversion results obtained with different random noise, we calculated the covariance matrices $\mathbf{C}^{12}$ and $\mathbf{C}^{45}$ for results obtained with equations (1) with (2) and (5) with (4), respectively. In order to simply compare the scatter of results of both types of the inversion, we calculated Euclidean norms of matrices $\mathbf{C}^{12}$ and $\mathbf{C}^{45}$, $\|\mathbf{C}^{12}\| = [\sum (c_{ij}^{12})^2]^{1/2}$ and $\|\mathbf{C}^{45}\| = [\sum (c_{ij}^{45})^2]^{1/2}$. All these calculations were performed for the noise levels of 1,2,3,4,5 and 10 ms. Figure 9 clearly demonstrates that application of the formula for c^{-1} (red) outperforms the more accurate formula for c^2 (blue). This can be simply explained by comparison of effects of noise in the right-hand sides of eqs (1) and (5). It is easy to show that for the choice of α_0 close to an average velocity, the effects of noise on the solution of eq. (1) are approximately twice as large as the effects of noise on the solution of eq. (5).

6 Conclusion and further plans

This contribution represents an attempt to study traveltime inversion in anisotropic media of arbitrary symmetry. As a first step, we used the VSP configuration, which provides good angular illumination of the medium and, thus, gives best chance to estimate most of parameters of the medium. We concentrated on P waves in a homogeneous, generally anisotropic medium. In the inversion scheme, we used approximate formulae for P waves, which are specified by 15 P-wave weak-anisotropy parameters in the case of most general anisotropy.

For data without noise, we got a perfect fit of inverted parameters with exact ones for a model with anisotropy of about 12%. For stronger anisotropy, specifically 25%, we got certain misfit. Obviously, the approximate formula for the P-wave ray velocity is not sufficiently accurate in this case.

Perhaps the most important observation is that addition of even very weak random noise leads to deviations of some inverted parameters from their exact counterparts. Application of the noise indicates significant instability of the inversion process. Estimations of some parameters vary considerably for varying realizations of the noise. Most prone to the mentioned deviations is WA parameter δ_z. On the other hand, very stable are parameters ϵ_z, ϵ_{34}, ϵ_{35} and χ_z. The explanation of this behaviour of the mentioned parameters is simple. Parameter δ_z is related to horizontal propagation (remember that the shallowest rays make about 26^o with the horizontal) while the remaining parameters are mostly related to vertical propagation (illumination of the model in the vertical direction is considerably better than in the horizontal direction).

Somewhat surprising is the result of the comparison of the use of formulae (2) and (4) in the inversion. Although eq. (4) represents, in fact, an approximation of (2), it seems to be more suitable for the inversion.

We plan to extend our present tests to estimate the limits of the experiment configuration in homogeneous media, below which there are low chances for the recovery of the parameters of the medium. In this respect, we plan to further reduce the number of shot profiles and the number of shots on them and study variations in the resolution of individual WA parameters. We also plan to extend the shot profiles in order to get better angular coverage close to horizontal. Although we do not expect a dramatic improvement in the inversion, we would like to test more accurate expressions for the ray velocity, see Farra and Pšenčík (2014), which take into account the deviations between ray-velocity and phase-velocity vectors. This specification will, however, lead to a system of nonlinear equations for WA parameters.

We would also like to study possibilities of the determination of anisotropic symmetry from the observed data. There are several possible ways how to attack this problem. We can try to invert the data assuming various symmetries of the medium and from the properties of the results to guess, which symmetry fits the data best. Such an approach was used, e.g., by Gomes et al. (2007). Another, similar approach was used by Seiner et al. (2010). We can also try to exploit the ideas proposed by Kelvin and revived and reviewed by Helbig (2013).

Our final and most difficult goal is to extend our studies to inhomogeneous media. We can expect that we shall face problems with instability and non-uniqueness. Thus, there will be a need for some kinds of regularization. Very probably, it will be necessary to reduce somehow the number of sought parameters as Chapman and Pratt (1992), Pratt and Chapman (1992), Mensch and Farra (2002) did. It might be also helpful to study situations when a partial information about considered structure is know from independent studies. An important stabilizing factor might be incorporation of S-wave traveltime data and P- and S-wave polarization data to the inversion.

Acknowledgement

We are grateful to project "Seismic waves in complex 3-D structures" (SW3D) and Research Project 210/11/0117 of the Grant Agency of the Czech Republic for support.

References

Backus,G.E., 1965. Possible forms of seismic anisotropy of the uppermost mantle under oceans. *J. geophys. Res.*, **70**, 3429-3439.

Červený, V., 1989. Ray tracing in factorized anisotropic inhomogeneous media. *Geophys. J. Int.*, **99**, 91-100.

Chapman, C.H., and Pratt, R.G., 1992. Traveltime tomography in anisotropic media - I. Theory. *Geophys. J. Int.*, **109**, 1–19.

Farra, V., and Pšenčík, I., 2014. Moveout approximations for P waves in media of monoclinic and higher anisotropy symmetries. *Seismic Waves in Complex 3-D Structures*, **24**, 35–58, online at "http://sw3d.cz".

Gajewski, D., and Pšenčík, I., 1990. Vertical seismic profile synthetics by dynamic ray tracing in laterally varying layered anisotropic structures. *J. Geophys. Res.*, **95**, 11301–11315.

Gomes, E.S., Pšenčík, I., Ball, G., 2007. Uncertainty in local determination of anisotropy parameters from a walkaway VSP. In: Seismic Waves in Complex 3-D Structures, Report 17, 63–77, Charles Univ. in Prague, Department of Geophysics.

Helbig, K., 2013. Review paper: What Kelvin might have written about Elasticity. *Geophys. Prosp.*, **61**, 1-20

Menke, W., 1984. *Geophysical data analysis: Discrete inverse theory.* Academic Press, New York.

Mensch, T., and Farra, V., 2002. P-wave tomography in inhomogeneous orthorhombic media. *Pure appl. geophys.* **159**, 1855-1879.

Pratt, R.G., and Chapman, C.H., 1992. Traveltime tomography in anisotropic media - II. Application. *Geophys. J. Int.*, **109**, 20–37.

Press, W.H., Flannery, B.P., Teukolsky, S.A., and Vetterling, W.T., 2007. *Numerical recipes.* Cambridge University Press, Cambridge.

Pšenčík, I., and Farra, V., 2005. First-order ray tracing for qP waves in inhomogeneous weakly anisotropic media. *Geophysics*, **70**, D65–D75.

Seiner, H., Bodnarova, L., Sedlák, P., Janeček, M., Srba, O., Král, R., and Landa, M., 2010. Application of ultrasonic methods to determine elastic anisotropy of polycrystalline copper processed by equal-channel angular pressing. *Acta Materialia*, **58**, 235–247.

Schoenberg, M., and Helbig, K. 1997, Orthorhombic media: Modeling elastic wave behavior in a vertically fractured earth. *Geophysics*, **62**, 1954–1974.

Thomsen, L., 1986. Weak elastic anisotropy. *Geophysics*, **51**, 1954–1966.

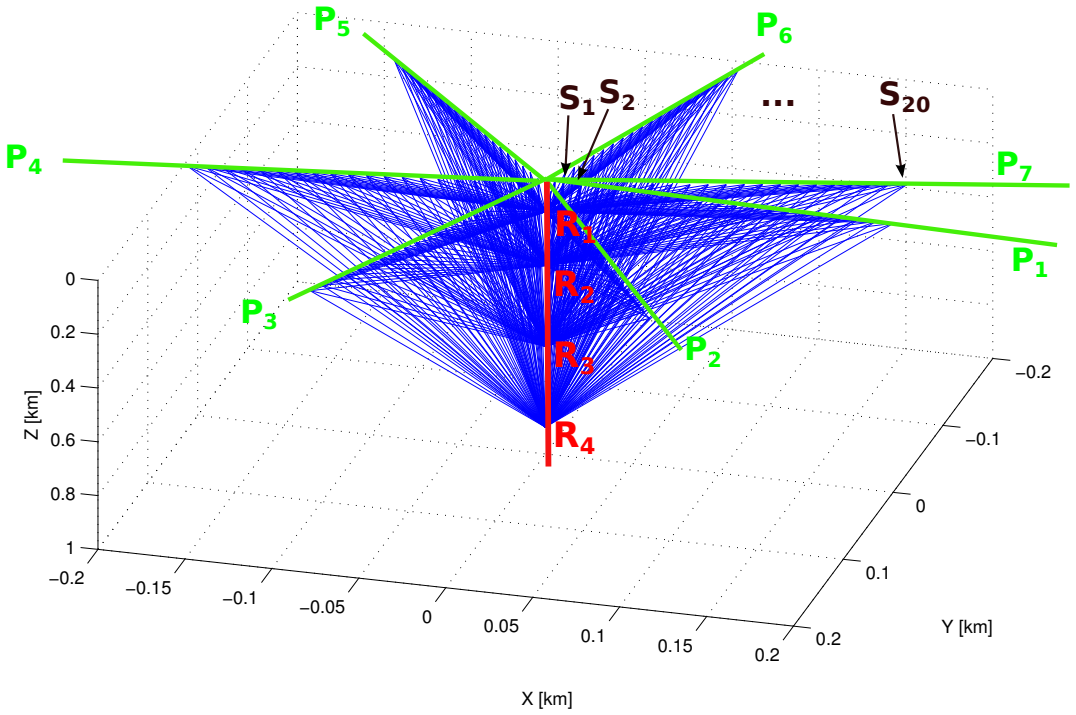

Figure 1: Configuration of the experiment with rays connecting 20 sources S_i (black) on each of 7 surface profiles P_i (green) with 4 receivers R_i (red) in the borehole.

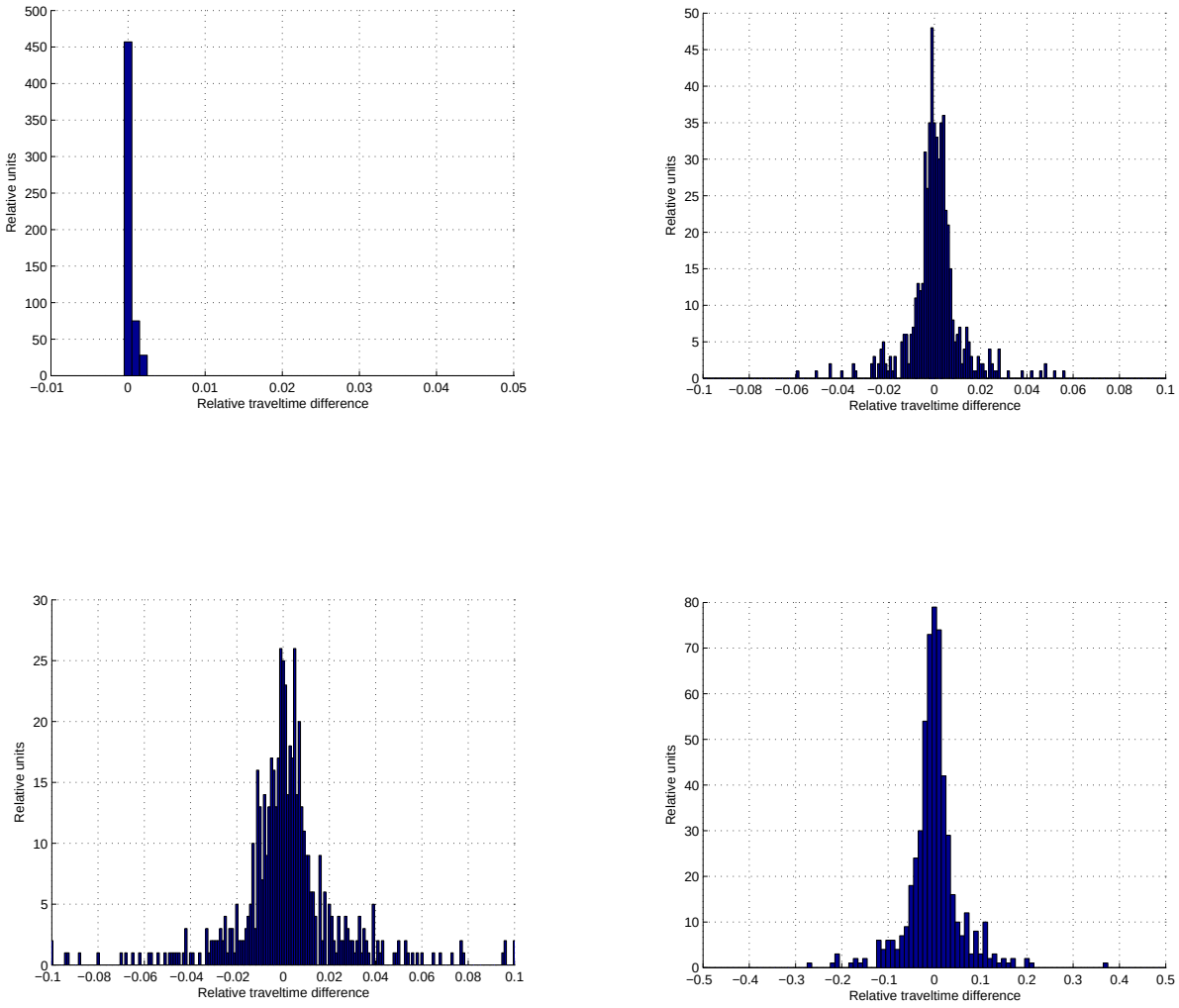

Figure 2: Relative traveltime mismodeling $(t_{obs} - t_{cal})/t_{cal}$ for Model A1. t_{obs} and t_{cal} - "observed" and calculated (from eq. (2)) traveltimes, respectively. The upper left: no noise; the upper right: random Gaussian noise 1 ms; the bottom left: 2 ms; bottom right: 5 ms. Note different scales on horizontal and vertical axes.

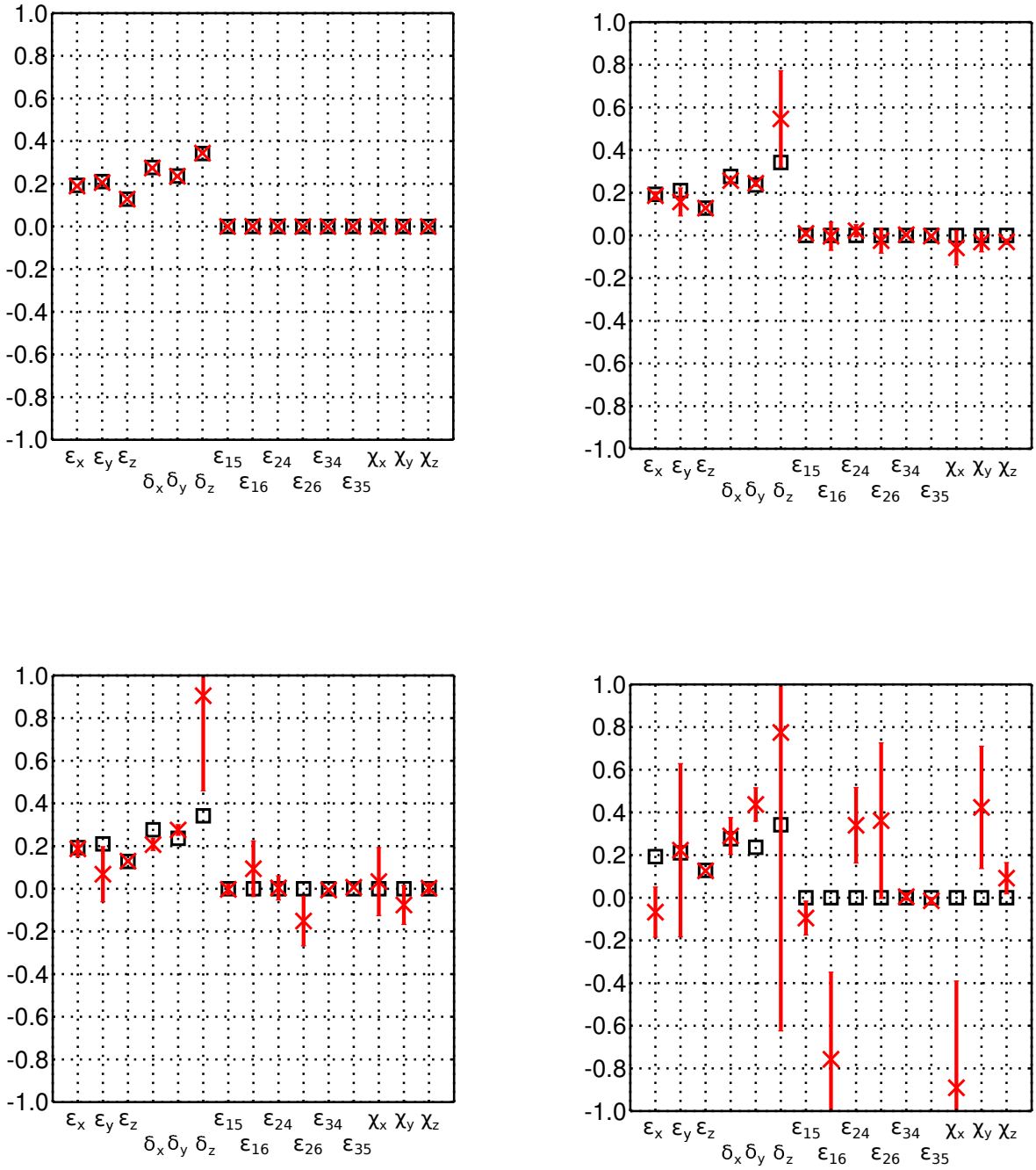

Figure 3: Results of inversion for Model A1. The upper left: no noise; the upper right: random Gaussian noise 1 ms; the bottom left: 2 ms; bottom right: 5 ms. Reference velocity: $\alpha_0 = 2.44$ km/s. Squares - exact values, red crosses - inverted values of WA parameters. Red bars indicate estimated errors of WA parameters.

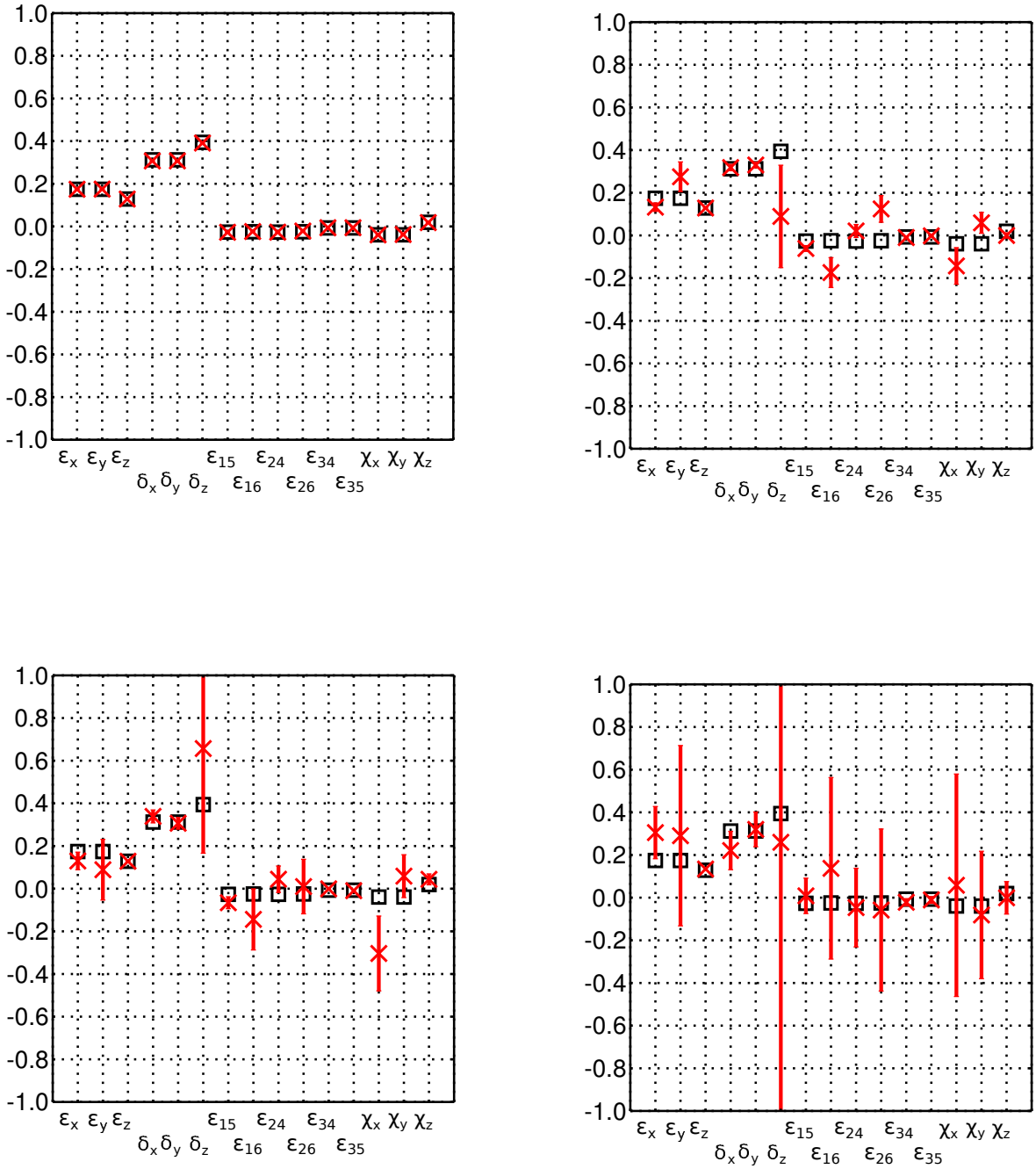

Figure 4: Results of inversion for Model A2. The upper left: no noise; the upper right: Random Gaussian noise 1 ms; the bottom left: 2 ms; bottom right: 5 ms. Reference velocity: $\alpha_0 = 2.44$ km/s. Squares - exact values, red crosses - inverted values of WA parameters. Red bars indicate estimated errors of WA parameters.

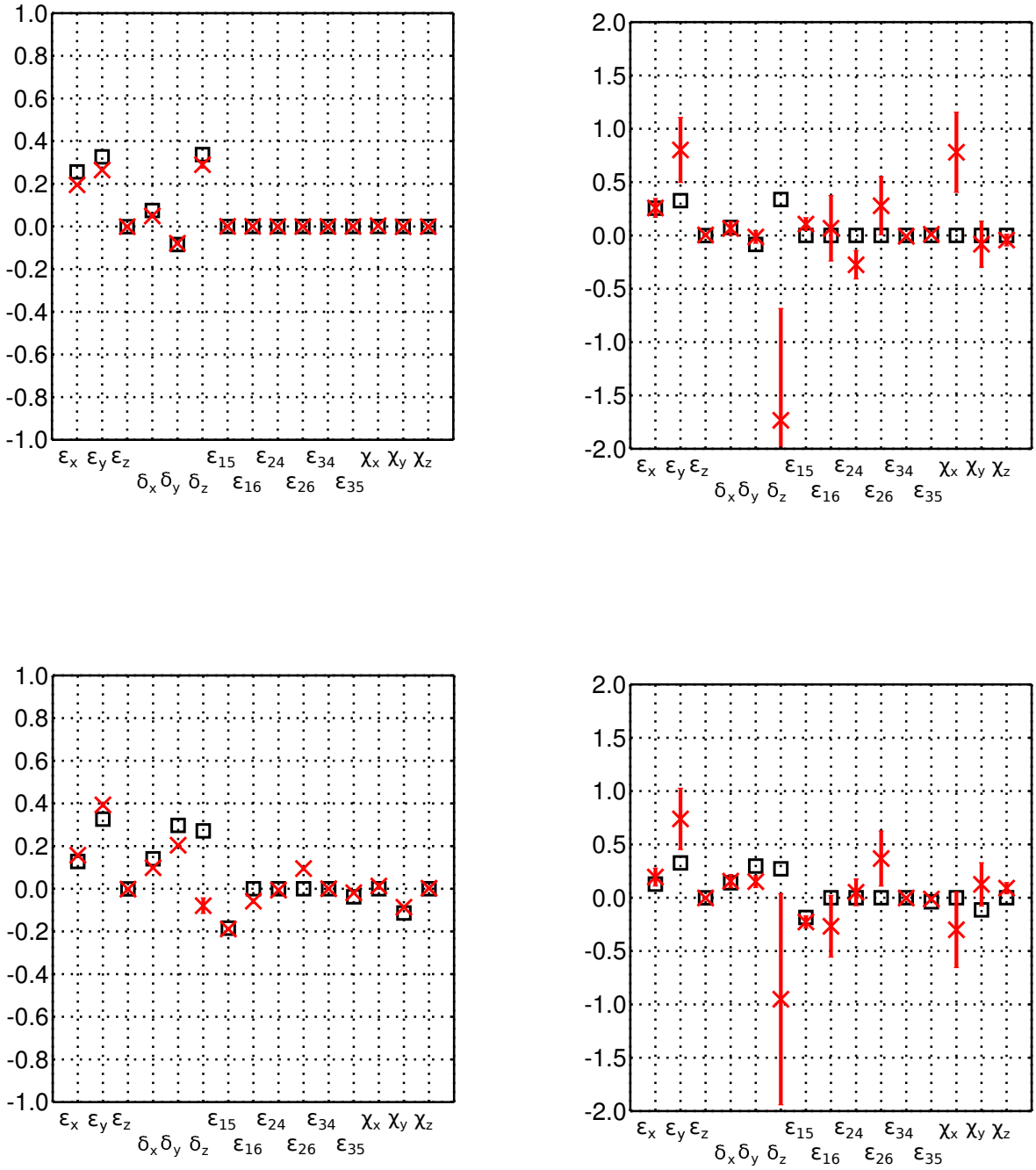

Figure 5: Results of inversion for Models A3 and A4. The upper left: Model A3, no noise; the upper right: Model A3, random Gaussian noise 5 ms; the bottom left: Model A4, no noise; bottom right: Model A4, Gaussian noise 5 ms. Reference velocity: $\alpha_0 = 2.44$ km/s. Squares - exact values, red crosses - inverted values of WA parameters. Red bars indicate estimated errors of WA parameters.

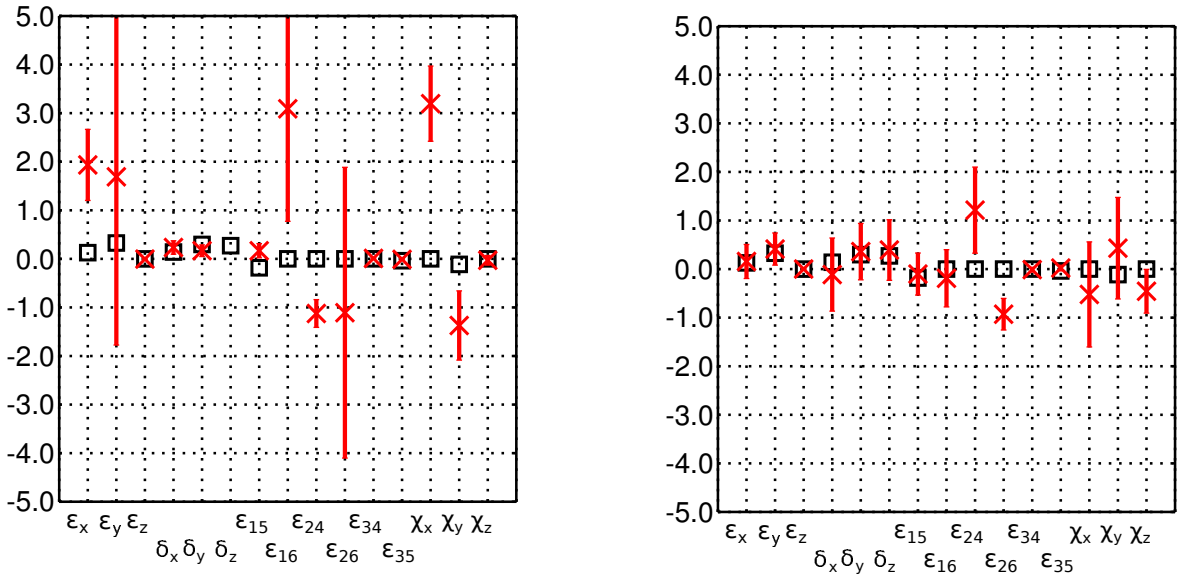

Figure 6: Results of inversion for Model A4, random Gaussian noise 5 ms. Left: data from receivers at depths of 0.3, 0.6 and 0.9 km considered; the receiver at the depth of 0.1 km omitted. Right: data from profiles with azimuths $\varphi = 0$, 2, 4 and 6 rad considered; remaining profiles omitted. Reference velocity: $\alpha_0 = 2.44$ km/s. Squares - exact values, red crosses - inverted values of WA parameters. Red bars indicate estimated errors of WA parameters.

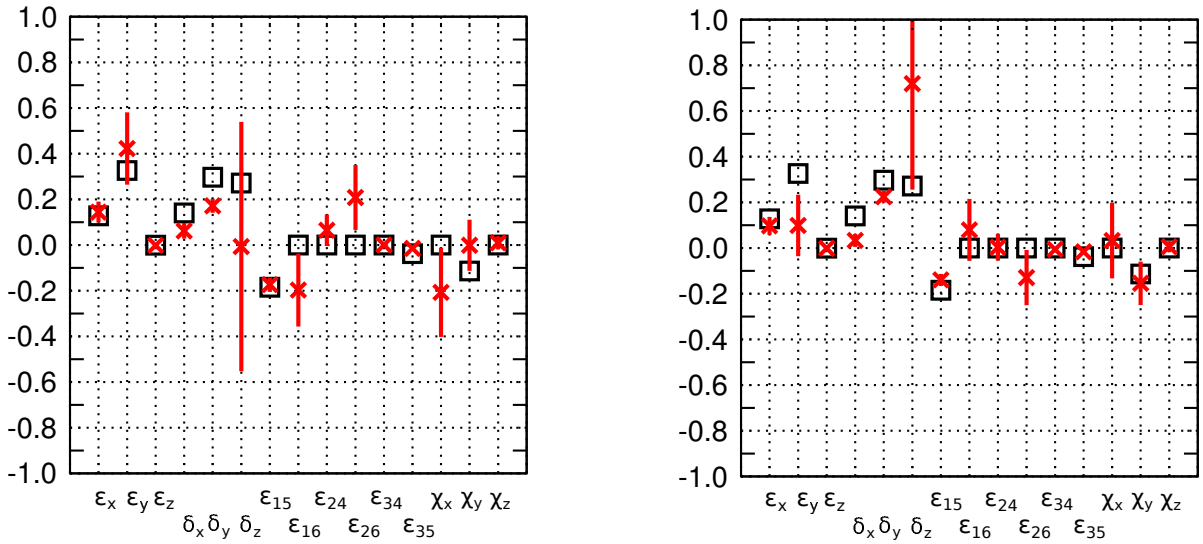

Figure 7: Results of inversion for Model A4, random Gaussian noise 3 ms. Left: results obtained from eq. (1) with $c^2(\mathbf{n})$ given in (2). Right: results obtained from eq. (5) with $c^{-1}(\mathbf{n})$ given in (4). Reference velocity: $\alpha_0 = 2.44$ km/s. Squares - exact values, red crosses - inverted values of WA parameters. Red bars indicate estimated errors of WA parameters.

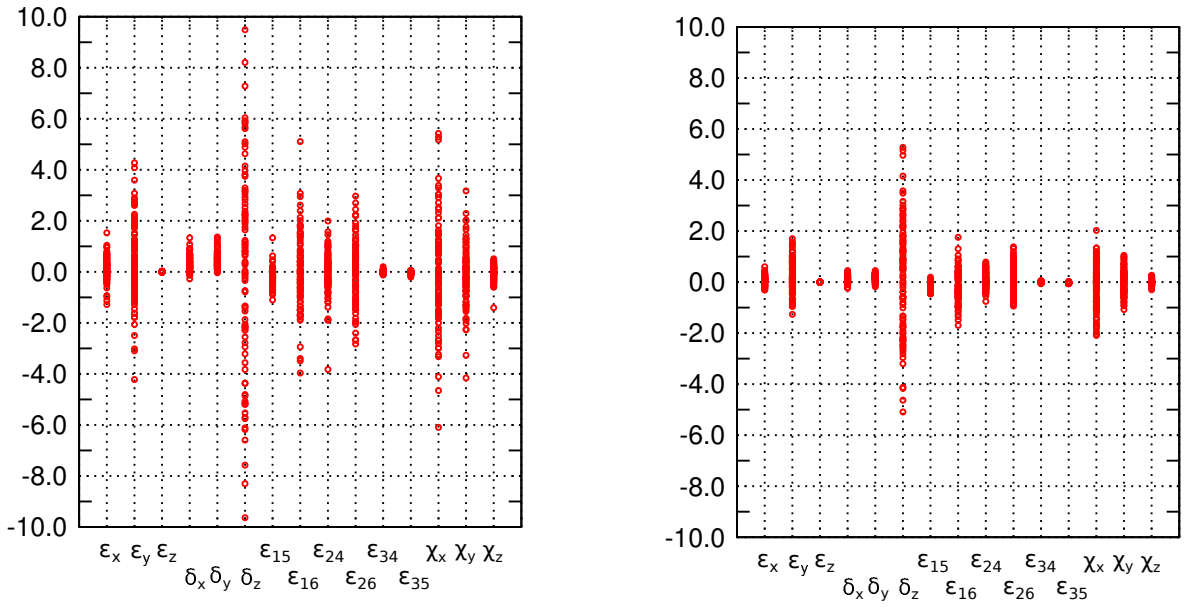

Figure 8: Results of inversion for Model A4, random Gaussian noise 10 ms, 100 realizations. Left: results obtained from eq. (1) with $c^2(\mathbf{n})$ given in (2). Right: results obtained from eq. (5) with $c^{-1}(\mathbf{n})$ given in (4). Reference velocity: $\alpha_0 = 2.44$ km/s. Red circles - inverted values of WA parameters.

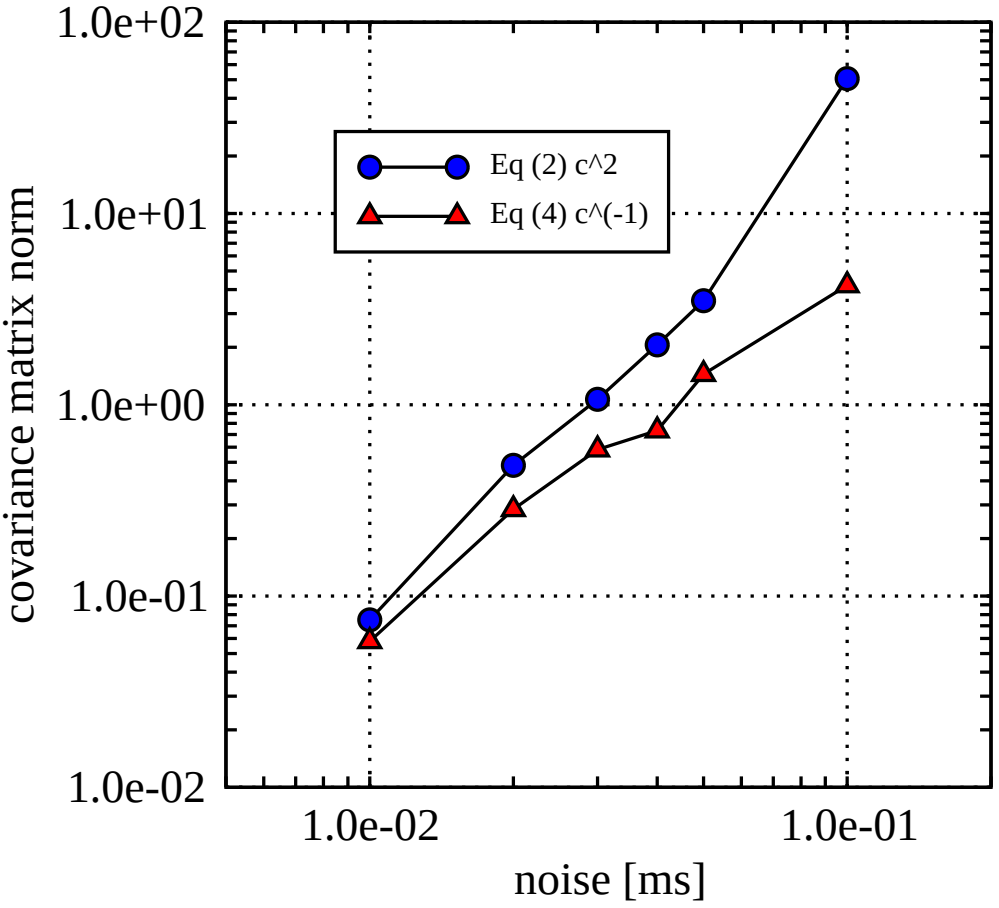

Figure 9: Covariance matrix norms for Model A4 calculated from 100 realizations for varying levels of random Gaussian noise (1,2,3,4,5 and 10 ms) for (1) with $c^2(\mathbf{n})$ given in (2) (blue) and for (5) with $c^{-1}(\mathbf{n})$ given in (4).